

The Monitoring and Control of GaP Thin Film Formation and Growth

Adam Attarian

May 8, 2006

1 Motivation

In the process of growing a thin film device via low pressure chemical deposition it is necessary to monitor and control the manufacturing process. Because of the incredibly small size of the structure, we must infer and monitor the growth based on the changing reflectivity's of optical sensors. Analyzing real-time thin film growth involves understanding the surface chemistry processes that control the film growth, such as composition, growth rate, and layer quality. Here we develop a model based upon a highly sensitive sensing technique which allows us to follow the surface reactions under steady-state growth conditions.

2 Properties of Reflection and Refraction

The reflection and refraction of light at a planar surface between two independent media with different dielectric properties ϵ_1 and ϵ_2 are well defined and characterized by the Fresnel Formulae. Specifically, the relative amplitudes of the reflective waves in the plane of incidence and perpendicular to the plane of incidence are given by

$$\frac{R_{1,p}}{A_{1,p}} = \frac{n_2 \cos \phi_1 - n_1 \cos \phi_2}{n_1 \cos \phi_1 + n_1 \cos \phi_2} = r_p$$

$$\frac{R_{1,s}}{A_{1,s}} = \frac{n_1 \cos \phi_1 - n_2 \cos \phi_2}{n_2 \cos \phi_1 + n_2 \cos \phi_2} = r_s$$

2.1 Snell's Law

Using Snell's Law of refraction, $n_1 \sin \phi_1 = n_2 \sin \phi_2$, we can show that the above Fresnel formulae can be expressed in the alternative forms

$$r_p = \frac{\tan(\phi_1 - \phi_2)}{\tan(\phi_1 + \phi_2)}$$

$$r_s = -\frac{\sin(\phi_1 - \phi_2)}{\sin(\phi_1 + \phi_2)}$$

First rewrite Snell's law as $n_2 = \frac{n_1 \sin \phi_1}{\sin \phi_2}$ and substitute into our original expression for r_p .

$$r_p = \frac{\frac{n_1 \sin \phi_1}{\sin \phi_2} \cos \phi_1 - n_1 \cos \phi_2}{\frac{n_1 \sin \phi_1}{\sin \phi_2} \cos \phi_1 + n_1 \cos \phi_2}$$

$$= \frac{\frac{n_1 \sin \phi_1 \cos \phi_1 - n_1 \sin \phi_2 \cos \phi_2}{\sin \phi_2}}{\frac{n_1 \sin \phi_1 \cos \phi_1 + n_1 \sin \phi_2 \cos \phi_2}{\sin \phi_2}}$$

$$= \frac{\sin \phi_1 \cos \phi_1 - \sin \phi_2 \cos \phi_2}{\sin \phi_1 \cos \phi_1 + \sin \phi_2 \cos \phi_2}$$

By using the identity $\cos^2 \phi_i + \sin^2 \phi_i = 1$,

$$r_p = \frac{\sin \phi_1 \cos \phi_1 [\cos^2 \phi_2 + \sin^2 \phi_2] - \sin \phi_2 \cos \phi_2 [\sin^2 \phi_1 + \cos^2 \phi_1]}{\sin \phi_1 \cos \phi_1 [\cos^2 \phi_2 + \sin^2 \phi_2] + \sin \phi_2 \cos \phi_2 [\sin^2 \phi_1 + \cos^2 \phi_1]}$$

$$= \frac{\sin \phi_1 \cos \phi_1 \cos^2 \phi_2 + \sin \phi_1 \cos \phi_1 \sin^2 \phi_2 - \sin \phi_2 \cos \phi_2 \sin^2 \phi_1 - \sin \phi_2 \cos \phi_2 \cos^2 \phi_1}{\sin \phi_1 \cos \phi_1 \cos^2 \phi_2 + \sin \phi_1 \cos \phi_1 \sin^2 \phi_2 + \sin \phi_2 \cos \phi_2 \sin^2 \phi_1 + \sin \phi_2 \cos \phi_2 \cos^2 \phi_1}$$

Multiplying the top and bottom of the above equation by $\frac{1}{\cos^2 \phi_1 \cos^2 \phi_2}$ and using the identity $\tan \phi_i = \frac{\sin \phi_i}{\cos \phi_i}$, we obtain

$$r_p = \frac{\tan \phi_1 + \tan \phi_1 \tan^2 \phi_2 - \tan^2 \phi_1 \tan \phi_2 - \tan \phi_2}{\tan \phi_1 + \tan \phi_1 \tan^2 \phi_2 + \tan^2 \phi_1 \tan \phi_2 + \tan \phi_2}$$

$$= \frac{(\tan \phi_1 - \tan \phi_2)(1 - \tan \phi_1 \tan \phi_2)}{(1 + \tan \phi_1 \tan \phi_2)(\tan \phi_1 + \tan \phi_2)}$$

So using the identity $\tan(\phi_i \pm \phi_j) = \frac{\tan \phi_i \pm \tan \phi_j}{1 \mp \tan \phi_i \tan \phi_j}$ we get the desired result

$$r_p = \frac{\tan(\phi_1 - \phi_2)}{\tan(\phi_1 + \phi_2)}.$$

We can also show that r_s can be rewritten as $r_s = -\frac{\sin(\phi_1 - \phi_2)}{\sin(\phi_1 + \phi_2)}$.

$$\begin{aligned}
r_s &= \frac{n_2 \frac{\sin \phi_2}{\sin \phi_1} \cos \phi_1 - n_2 \cos \phi_2}{n_2 \frac{\sin \phi_2}{\sin \phi_1} \cos \phi_1 + n_2 \cos \phi_2} \\
&= \frac{\frac{\sin \phi_2}{\sin \phi_1} \cos \phi_1 - \cos \phi_2}{\frac{\sin \phi_2}{\sin \phi_1} \cos \phi_1 + \cos \phi_2} \\
&= \frac{\sin \phi_2 \cos \phi_1 - \sin \phi_1 \cos \phi_2}{\sin \phi_2 \cos \phi_1 + \sin \phi_1 \cos \phi_2}
\end{aligned}$$

So by using the identity $\sin(\phi_i \pm \phi_j) = \sin \phi_i \cos \phi_j \pm \cos \phi_i \sin \phi_j$ we can conclude that

$$r_s = -\frac{\sin(\phi_1 - \phi_2)}{\sin(\phi_1 + \phi_2)}$$

We note that the denominator in r_p is finite except when $\phi_1 + \phi_2 = \pi/2$, in which case $\tan(\phi_1 + \phi_2) = \infty$. When this happens we see that $r_p = 0$ and consequentially $\tan \phi_1 = \frac{n_2}{n_1}$.

Since we know $\phi_1 + \phi_2 = \frac{\pi}{2} \Rightarrow \phi_1 = \frac{\pi}{2} - \phi_2$ and by Snell's Law $\frac{n_2}{n_1} = \frac{\sin \phi_1}{\sin \phi_2}$ we can conclude the following

$$\begin{aligned}
\tan \phi_1 &= \frac{\sin \phi_1}{\cos \phi_1} \\
&= \frac{\sin \phi_1}{\cos(\frac{\pi}{2} - \phi_2)} \\
&= \frac{\sin \phi_1}{\sin \phi_2} \\
&= \frac{n_2}{n_1}
\end{aligned}$$

Lastly, since $\phi_1 + \phi_2 = \pi/2$, and $\phi_1 = \phi'_1$ by definition, then the complement to $\phi'_1 = \phi_2$ and $\phi_4 = \pi/2 - \phi_2$, ϕ_5 , the angle between the x-axis and the transmitted ray in the second quadrant, therefore $\phi'_1 + \phi_5 = \phi_1 + \phi_2 = \pi/2$, and so we see the reflected and transmitted rays are orthogonal.

2.2 Brewster's Angle

The angle ϕ_1 such that $\tan \phi_1 = \frac{n_2}{n_1}$ is referred to as the Brewster Angle, and is the angle at which the electric vector has no component in the plane of incidence. This is equivalent to saying that the light is then polarized "in the plane of incidence." For glass, the refractive index $\frac{n_2}{n_1}$ is 1.52, or approximately 57° . We can verify this by plotting the values of r_p and r_s as a function of $\phi_1 \in [0, 90^\circ]$.

We notice that $r_p = 0$ at close to 57° , and so the Brewster angle does indeed correspond to the polarizing angle $\tan \phi_1 = 1.52$

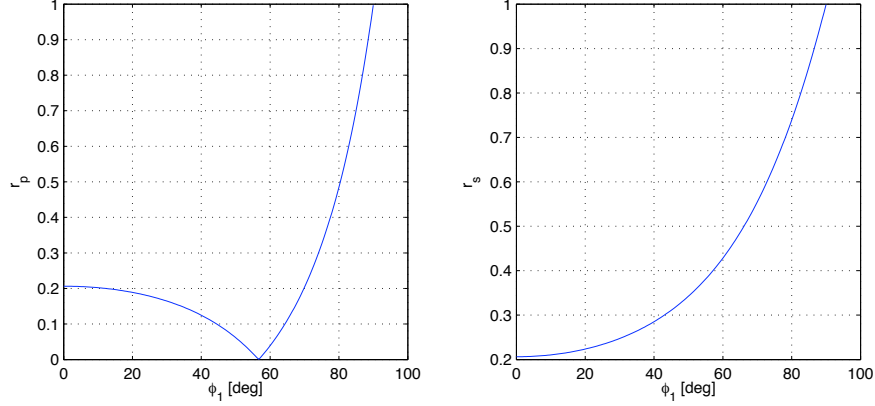


Figure 1: Reflection Coefficients Versus ϕ_1

3 Model Simulation

In the problem we consider a four layer stack consisting of the ambient medium, a surface reaction layer, an epitaxial film, and a substrate. The surface reaction layer is composed of molecules, molecular fragments, and atoms that are generated on the surface of the solid by pyrolysis of the source vapor molecules and the resulting chemical reactions.

The model for the complex reflectivity coefficient for a four-layer stack is given by

$$r_p = \frac{r_{12}(1 + r_{23}r_{34}e^{-2i\beta_3}) + (r_{23} + r_{34}e^{-2i\beta_3})e^{-2i\beta_2}}{(1 + r_{23}r_{34}e^{-2i\beta_3}) + r_{12}(r_{23} + r_{34}e^{-2i\beta_3})e^{-2i\beta_2}}$$

where the Fresnel coefficients $r_{k(k+1)}$, $k = 1, 2, 3$ for the interfaces 12, 23 and 34 are given by

$$r_{k(k+1)} = \frac{\epsilon_{k+1}\sqrt{\epsilon_k - \epsilon_1 \sin^2 \phi_1} - \epsilon_k\sqrt{\epsilon_{k+1} - \epsilon_1 \sin^2 \phi_1}}{\epsilon_{k+1}\sqrt{\epsilon_k - \epsilon_1 \sin^2 \phi_1} + \epsilon_k\sqrt{\epsilon_{k+1} - \epsilon_1 \sin^2 \phi_1}}$$

and the phase angles β_k for the srl ($k = 2$) and the growing epilayer ($k = 3$) are given by

$$\beta_k = \frac{2\pi}{\lambda} d_k \sqrt{\epsilon_k - \epsilon_1 \sin^2 \phi_1}$$

where d_k , $k = 2, 3$ refer to the thicknesses of the SRL and epilayer, respectively and $\epsilon_1, \epsilon_2, \epsilon_3, \epsilon_4$ refer to the dielectric functions of the ambient, SRL, epilayer, and substrate respectively at wavelength λ of the incident laser beam. The values for ϵ_3 and ϵ_4 have been

estimated to fit the large interference. For our model, the following values were defined.

λ	632.8nm
ϵ_1	1
ϵ_3	$10.6915 - 0.0016i$
ϵ_4	$15.3171 - 0.1771i$
ϕ_1	75.26°

This leaves ϵ_2 , d_2 and d_3 to be determined to find r_p . In the vapor deposition process, the source emits a constant flux of tertiary-butylphosphine(TBP), followed by a pause, then a constant flux pulse of triethylgallium(TEG), followed by a pause before the beginning of the next cycle. A series of chemical reactions occur to create the gallium phosphide (GaP) film. These reactions can be approximated by a series of ordinary differential equations, given by

$$\begin{aligned} \frac{d}{dt}n_1(t) &= S_1(t) - k_1n_1(t) - k_{GaP}n_1(t)n_3(t), \\ \frac{d}{dt}n_2(t) &= S_2(t) - k_2n_2(t) - k_3n_2(t), \\ \frac{d}{dt}n_3(t) &= k_3n_2(t) - k_4n_3(t) - k_{GaP}n_1(t)n_3(t), \\ \frac{d}{dt}n_4(t) &= k_{GaP}n_1(t)n_3(t). \end{aligned}$$

The variables n_1 , n_2 and n_3 represent the number of moles of the components of the srl (phosphorus(P), monoethylgallium(MEG) and gallium(Ga) respectively). In the first equation the change in P is described by the source term S_1 , the desorption loss term $-k_1n_1$ and the reaction term forming GaP. The second equation, which describes the defragmentation of TEG, contains the source term S_2 , a desorption loss term $-k_2n_2$ and a term of decomposition into MEG and active gallium fragments. The third equation (change in MEG and active surface gallium fragments) has the reaction term of creation from MEG, a desorption loss term and the reaction term forming GaP. In addition to these three variables, n_4 represents the number of moles of the GaP film. Its equation contains only the reaction term of formation of GaP from Ga and P. The source terms are based on the source vapor pulses, and are given by

$$\begin{aligned} S_1(t) &= \frac{P_1(t)}{V_{TBP}}\gamma\beta_{TBP} \\ S_2(t) &= \frac{P_2(t)}{V_{TEG}}\gamma\beta_{TEG} \end{aligned}$$

where γ is how much of the source vapors will actually reach the surface, and β_{TBP} is the sticking coefficient of TBP. For each source term we are using a constant flow rate between

the start and stop times. There is a small time difference between the switching on and off of the pulse and the start and stop of the source vapors at the surface. Because of this, we add a delay parameter, t_d so we estimate that the source vapors reach the surface starting at $t_0 + t_d$ and stopping at $t_f + t_d$. The value of t_d will be estimated.

Once the differential equations have been solved with an iterative method such as `ode23` we can solve for unknown values ϵ_2 , d_2 and d_3 . To solve the ODE's using `ode23`, we first scaled up the equations by a factor of 10^8 , and then after solving scale them back down by 10^{-8} . This ensures minimizing computational and other round-off error. The film and SRL thicknesses are then given by

$$\begin{aligned} d_3 &= \frac{1}{A}n_4V_{GaP} + (d_3)_0, \\ d_2 &= \frac{\alpha_{SRL}}{A}[n_1V_1 + n_2V_2 + n_3V_3], \end{aligned}$$

The effective dielectric function of the srl will be defined by

$$\epsilon_2 = \epsilon_\infty + \alpha \left[\frac{n_1}{\sum_{k=1}^3 n_k} F_1 + \frac{n_2}{\sum_{k=1}^3 n_k} F_2 + \frac{n_3}{\sum_{k=1}^3 n_k} F_3 \right].$$

where A is the surface area of the wafer, V_i is the molar volume of the component n_i and V_{GaP} is the molar volume of GaP. The parameters F_i are the optical responses of the SRL components, and ϵ_∞ and α are constants, which are both considered 1 for this problem. α_{SRL} is an effective SRL thickness parameter representing the percentage of the SRL that contributes to the reflectance behavior and is taken to be 0.75. The value for $(d_3)_0$ is the initial film thickness, and is known to be 252 angstrom. With these parameters, the complex reflectivity coefficient r_p can be found, as well as the reflectance, defined as $R_p = |r_p|^2$

For our first model run, we will presume the following input values: a cycle length of 3 seconds, with the first pulse between 0.0 and 0.8 seconds and the second pulse's starting and ending times are 1.3 and 1.6 seconds respectively.; the source vapor flow rates $P_1 = 0.907cm^3/min$ and $P_2 = 0.04cm^3/min$; the molar volumes $V_{TBP} = 128.57cm^3/mole$, $V_{TEG} = 148.36cm^3/mole$, $V_1 = 17.02cm^3/mole$, $V_2 = 13.00cm^3/mole$, $V_3 = 11.81cm^3/mole$, and $V_{GaP} = 12.19cm^3/mole$; the sticking coefficients $\beta_{TBP} = 0.15$ and $\beta_{TEG} = 1.0$; and a circular wafer with a 2in diameter. Use the approximate parameters $F_1 = 15 - 1i$, $F_2 = 15 - 0.5i$, $F_3 = 14 - 5i$, $k_1 = 4$, $k_2 = 2.0$, $k_3 = 4.0$, $k_4 = 0.1$, $k_{GaP} = 2$, $\gamma = 0.06$ and $t_d = 0.5$. The reflectance was then calculated over 4 periods of deposition, resulting in a run 12 seconds long.

3.1 Model Results

Running the code on a 12 second run with the model parameters produced the following plots of results.

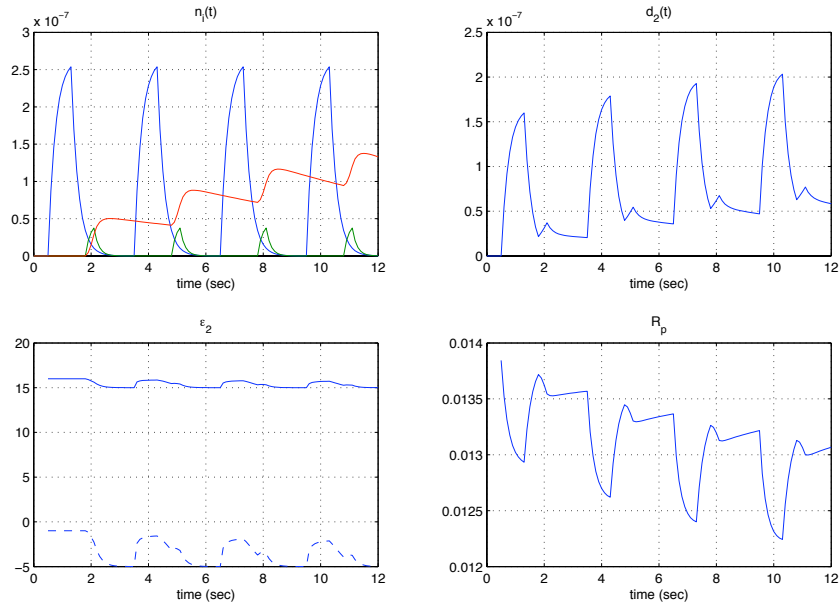


Figure 2: Model Based Results: n_i , SRL thickness, Dielectric Function, General Reflectance

In addition, $n_4(t)$ was calculated to be

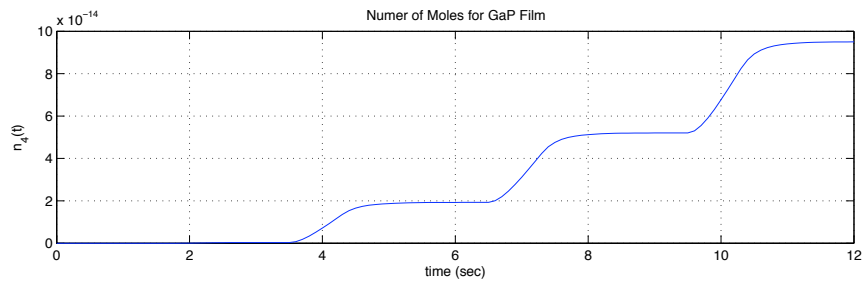


Figure 3: GaP moles versus time

We note the periodicity of the formation with the 3 second interval. In addition, due to the low k_4 term, we have $n_3(t)$ not decaying with the interval. We found through testing that k_4 needs to be in the neighborhood of 2 in order to produce consistently decaying

results for $n_3(t)$. We can compare this simulation to collected experimental data over a similar time interval. In doing so, we have the convenience of being able to ignore phase and amplitude differences, and instead can compare the shape of the data. We can do this because over a long period of time, the model produces a relatively low frequency, where the actual reflectance data is similar to high frequency noise riding atop the sine wave. This said, we can arbitrarily “zoom in” on the sinusoidal experimental data and find the data that matches our temporal location in the experiment. The timing information for the experimental data is based on the n^{th} time sample by the DSP. The DSP has a Δt interval of .01 seconds.

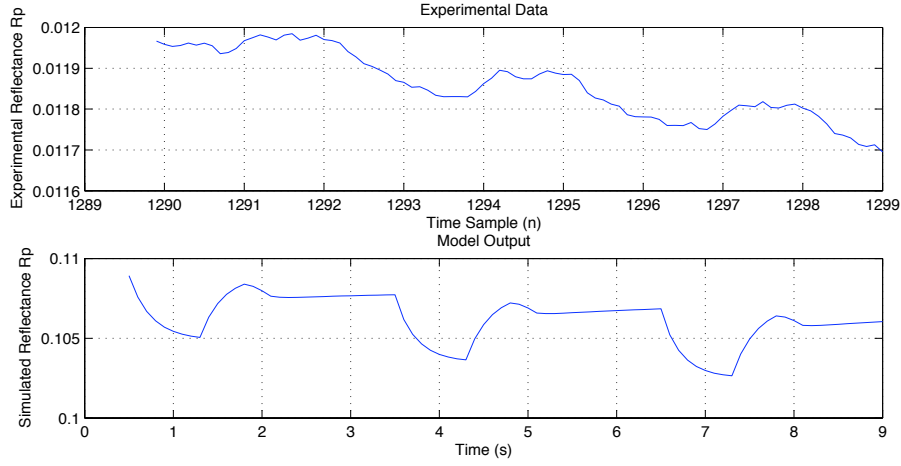


Figure 4: Model Data versus Experimental Data

The experimental data was collected at a different scaling than our model produces, so we scaled the data down by 984 to produce more realistic results. There are good similarities between our experiment on the chosen time interval and our model. Generally, the shapes match when the presence of additive white gaussian noise is taken into account. The general rise and fall of the data match. Additionally, we found the average dielectric function to have a value of $15.4197 - 3.2927i$, with an average growth of $9.6014\text{E-}015$ cm/second, computed via a standard linear regression. We should note that the experimental data does not reflect the presence of a timing delay, which explains the absence of correlation at the earliest time samples.

It is a relief that the general shape and trend of the data matches our result. We see the vapor deposition being periodic with the time interval of three seconds, and the general upward and downward trends corresponding to the same relative times.

3.2 Optimal Parameters

In order to find a set of physical realizable parameters to conform our model to collected data, there must be a way to measure how the two data sets are apart. One method to do this is via the well defined inverse least squares method. We will define the cost function J

$$J = \sqrt{\sum_t (R_{exp}(t) - R_{calc}(t))^2}$$

Minimizing the cost function J will reveal which parameters for which R_{calc} will be closest to the experimental reflectance R_{exp} . Minimizing the cost function J is out of the scope of this paper due to the computational challenge and other minimization intricacies, however we can use the values given in the paper “*Representation of GaP formation by a reduced order surface kinetics model using p-polarized reflectance measurements*”, J. of Applied Physics, vol. 86, no. 1, 1999 (S. Beeler, H.T Tran, and N. Dietz). The optimal parameters reported in the paper were

$$\vec{q} = \begin{bmatrix} k_1 \\ k_2 \\ k_3 \\ k_4 \\ k_{GaP} \\ F1 \\ F2 \\ F3 \\ t_d \end{bmatrix} = \begin{bmatrix} 3.31 \\ 1.55 \\ 2.14 \\ 0.052 \\ 2.0 \\ 13.46 - 0.13i \\ 13.56 - 0.0i \\ 19.36 - 11.02i \\ 0.72 \end{bmatrix}$$

Using \vec{q} as the input parameters to our model, we arrive with the following results in Figure 5.

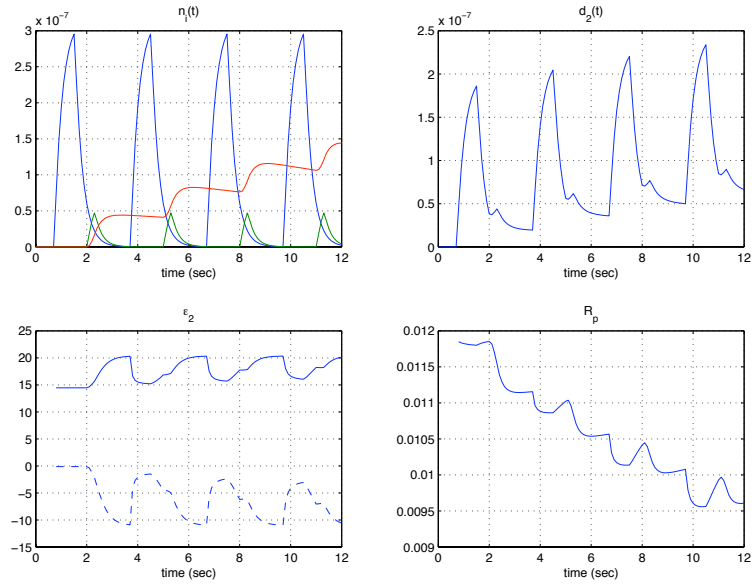


Figure 5: Optimal Input Parameter Model Output

Additionally, $n_4(t)$ was determined to be the function presented in Figure 6.

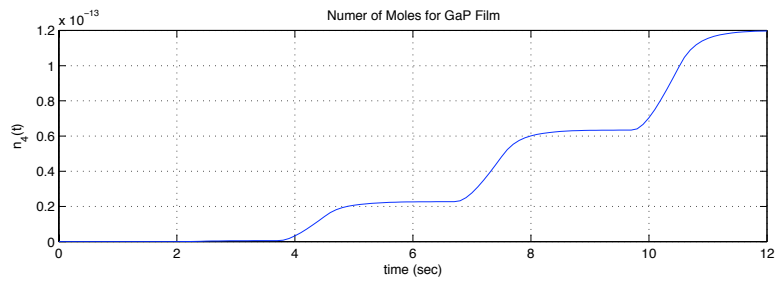


Figure 6: GaP Moles versus time (optimal parameters)

Lastly, matching our model output to experimental data, we see the correlation presented in Figure 7.

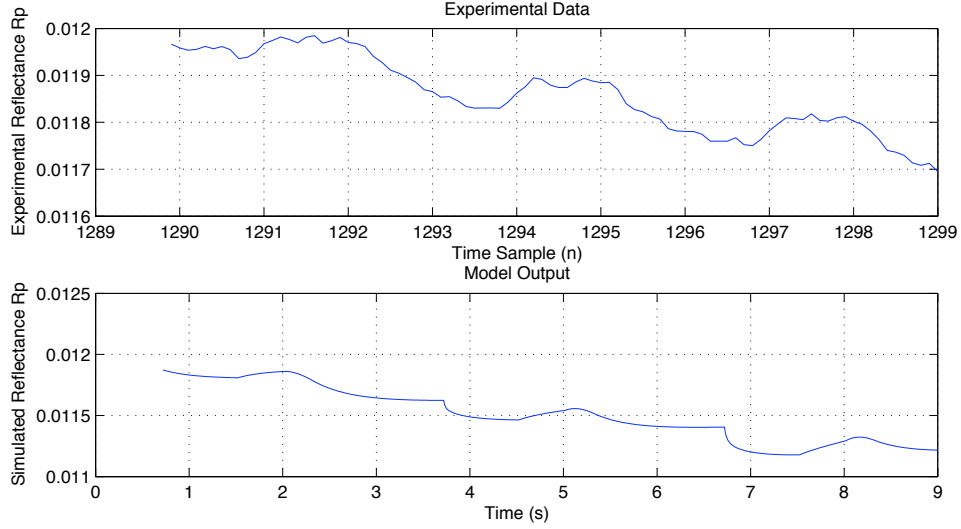


Figure 7: GaP Moles versus time (optimal parameters)

When comparing the two data sets, we still a match in the general trend of the data. Comparing the optimal and non-optimal parameter sets, it appears that both the non-optimal parameters and optimal parameters produce results which match the experimental set in a qualitative manner. The optimal parameters have a consistently decaying trend over the interval, and this is also reflected in the data. We found the dielectric function to have an average value of $17.3595 - 5.456i$, with an average growth of $1.1306E-014$ cm/second.

3.3 Variation of Parameters

We varied individual parameters of the model to see what effect it would have on the output. The respective plots are omitted for brevity, however a qualitative description of the results should suffice.

1. $k_{3,new} = k_3/10$

- n_1 : no apparent change
- n_2 : increased amplitude, identical shape
- n_3 : decreased amplitude, identical shape
- n_4 : decreased amplitude, identical shape
- d_2 : decreased amplitude, slope decreased
- ϵ_2 : slope less negative, shape different
- R_p : slope less negative, shape different

2. $\Re(F_{3,new}) = \Re(F_3/10)$

- n_1, n_2, n_3, n_4 : no change, mathematically independent
- d_2 : no apparent change
- ϵ_2 : increased amplitude, same shape overall
- R_p : shape different, positive slope.

3. $\Im(F_{3,new}) = \Im(F_3/10)$

- n_1, n_2, n_3, n_4 : no change, mathematically independent
- d_2 : no apparent change
- ϵ_2 : no apparent change
- R_p : decreased amplitude, shape change to a more positive general slope

4. $\Im(\epsilon_{3,new}) = \Im(\epsilon_3/10)$

- n_1, n_2, n_3, n_4 : no change, mathematically independent
- d_2 : no apparent change
- ϵ_2 : decrease to negative range
- R_p : no apparent change

3.3.1 A Case of Interest

In the referenced paper, it is evident that $n_3(t)$ is decaying over the period. We found this puzzling, as with both the problem and optimal parameters $n_3(t)$ was increasing over all time intervals. We were curious to see what change in model parameters could reproduce the plot given in the paper. Through trial and error runs, we found that the plot could be reproduced when the parameter k_4 was in the neighborhood of 2. Using this value, with all other values being the problem parameters, produces the following plots. We see that the GaP film growth is slower over time, and that the overall reflectance has a better fit with the plots offered in the paper.

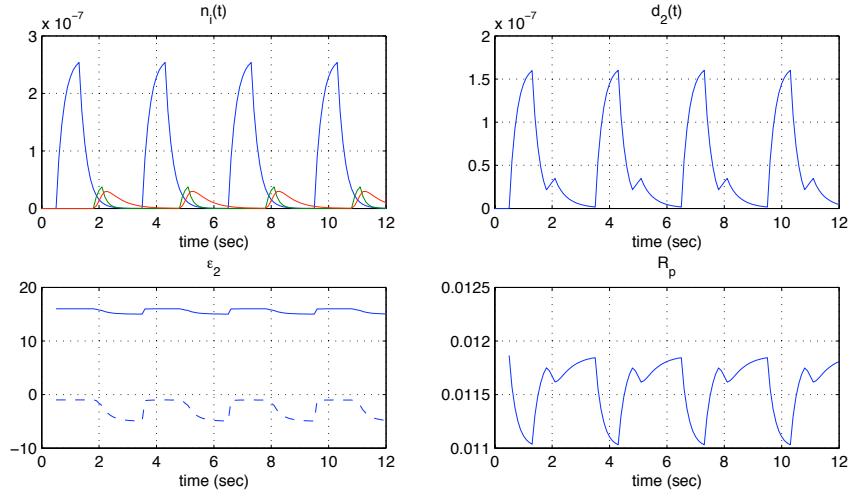


Figure 8: Model Output with $k_4=2$

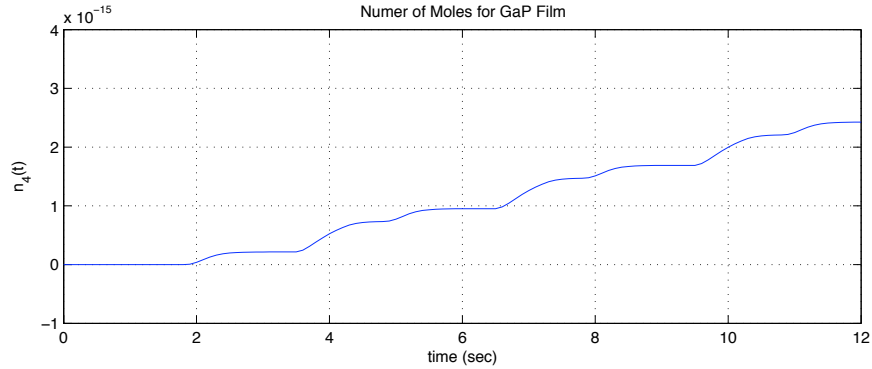


Figure 9: GaP growth with $k_4=2$

4 Discussion and Conclusion

The model for the thin film growth formation of GaP is very complex, and contains many subtleties and only what can best be called idiosyncrasies. We had to consistently be concerned with the computational considerations of the problem, given the magnitude of the solution space that we were working in. For the first time, how we used the numerical ODE solver became important.

The model was simulated in MATLAB using both problem parameters and optimal parameters given in the paper. A sensitivity analysis was performed to study the effect of the pertinent parameters. Both simulations were compared to an experimental data set and the correlations were discussed. Finally, we note that amplitudes and time-averaged behavior for a selected, arbitrary interval were a close fit, however the numerical model failed to capture the noise and variation evident in the experimental data.